Physicochemical and morphological characterisation of nanoparticles from photocopiers: Implications for environmental health

Article *in* Nanotoxicology · May 2012

Impact Factor: 6.41 · DOI: 10.3109/17435390.2012.689883 · Source: PubMed

Nanotoxicology, 2012; Early Online, 1–15

ISSN: 1743-5390 print / 1743-5404 online
DOI: 10.3109/17435390.2012.689883

informa
healthcare

Physicochemical and morphological characterisation of nanoparticles from photocopiers: implications for environmental health

Dhimiter Bello[1], John Martin[1], Christopher Santeufemio[1], Qingwei Sun[2], Kristin Lee Bunker[3], Martin Shafer[4], & Philip Demokritou[2]

[1]*University of Massachusetts Lowell, One University Avenue, Lowell, MA, USA,* [2]*Harvard School of Public Health, 401 Park Drive, Boston, MA, USA,* [3]*R J Lee Group, Inc., Monroeville, PA, USA and* [4]*Wisconsin State of Hygiene Laboratory, 2601 Agriculture Drive, Madison, WI, USA*

Abstract

Several reports link printing and photocopying with genotoxicity, immunologic and respiratory diseases. Photocopiers and printers emit nanoparticles, which may be involved in these diseases. The physicochemical and morphological composition of these emitted nanoparticles, which is poorly understood and is critical for toxicological evaluations, was assessed in this study using both real-time instrumentation and analytical methods. Tests included elemental composition (40 metals), semi-volatile organics (100 compounds) and single particle analysis, using multiple high-sensitivity/resolution techniques. Identical analyses were performed on the toners and dust collected from copier's exhaust filter. Engineered nanoparticles, including titanium dioxide, iron oxide and fumed silica, and several metals were found in toners and airborne nanoscale fraction. Chemical composition of airborne nanoscale fraction was complex and reflected toner chemistry. These findings are important in understanding the origin and toxicology of such nanoparticles. Further investigation of their chemistry, larger scale exposure studies and thorough toxicological characterisation of emitted nanoparticles is needed.

Keywords: Nanoparticles, printers, photocopiers, toner, environmental health, nanotoxicology

Introduction

Printers and photocopiers have become an integral part of modern life and accompany us at homes, offices and other indoor environments. The printing and photocopying technology has been scrutinised in the past because of its association with indoor air pollutants, especially particulate matter (PM), ozone and volatile organic compounds (VOCs) (Lee & Hsu 2007; Tuomi et al. 2000; Destaillats et al. 2008). More recently, consumer-grade printers have been the subject of much public controversy, especially in countries like Germany and Australia, this time because of emission of high concentrations of nanoparticles (NP, definition and terminology defined later in the introduction) (Morawska et al. 2009; Kagi et al. 2007; He et al. 2007; Schripp et al. 2008; McGarry et al. 2011). This work revealed that emissions are highly variable and depend on a host of poorly understood factors such as printer's manufacturer and model, printer age, fuser temperature, page coverage and printing frequency (Morawska et al. 2009; He et al. 2007; Schripp et al. 2008; He et al. 2010). Nanoparticles from printers seem to be formed primarily from the condensation of semi-volatile organic compounds (SVOCs), evaporated from the toner during the printing process and include different classes of poorly characterised organic compounds, such as alkanes, siloxanes and other higher boiling point constituents (Morawska et al. 2009; Wensing et al. 2009). Recently, Barthel et al. (2011) reported for the first time on emission of other elements of an inorganic origin, including silicon (Si), sulphur (S) and several metals such as titanium (Ti), iron (Fe), chromium (Cr), nickel (Ni) and zinc (Zn). They estimated that solid inorganic particles accounted for <2% of the total number of emitted nanoparticles and originated from toner, paper and plastic housing.

Much less is known about emissions and personal exposures to nanoparticles generated by commercial photocopiers. To date no reports exist on the chemical composition of these nanoparticles. Photocopying can emit significantly more nanoparticles than printers due to their high output and continuous mode of operation. In addition, photocopiers are housed sometimes in small rooms without sufficient ventilation with peak particle number concentrations reported at 1×10^8 particles/cm^3 (Lee & Hsu 2007). Since photocopiers are often located in common areas in many businesses and used by many, NP exposures from

Correspondence: Dhimiter Bello, University of Massachusetts Lowell, One University Avenue, Lowell, MA 01854, USA and Philip Demokritou, Harvard School of Public Health, 401 Park Drive, Boston, MA 02215, USA. Tel: + 1 978 934 3343. Fax: +978 452 5711.
E-mail: dhimiter_bello@uml.edu; pdemokri@hsph.harvard.edu

(Received 15 December 2011; accepted 26 April 2012)

photocopiers may represent both an occupational and public health issue.

A brief definition of some frequently used terms is provided for clarity. A more comprehensive description of these terms can be found in Lövestam et al. (2010). The term 'nanoparticle' refers to particles with three dimensions in the nanoscale (1–100 nm) range. When nanoparticles are generated as unintended by-products of industrial or anthropogenic activities (e.g. diesel exhaust or welding fumes), they are generally called incidental nanoparticles. By contrast, engineered nanoparticles are intentionally produced to fulfil desired technological functions (e.g. carbon black or titanium dioxide). The term 'ultrafine particles', common in the air pollution field, is synonymous with incidental nanoparticles. The term nanomaterial is used to describe a substance comprising particles, the substantial majority of which have three dimensions of the order of 100 nm or less. In this manuscript, the term 'nanoparticles' and ultrafine particles are used interchangeably to mean incidental nanoparticles to distinguish them from engineered nanoparticles. Similarly, we will use nanomaterial (NM) for those of incidental origin and engineered NMs for the manufactured ones (Lövestam et al. 2010). Based on these definitions, nanoparticles emitted from printers and photocopiers are incidental nanoparticles. However, if engineered nanoparticles were used in the toners and some of them would become airborne, this would result in a mixture of both incidental and engineered nanoparticles. The familiar term 'airborne particulate matter' refers to broad particle size distributions in air (1 nm to at least 10 μm).

The toxicological significance of such particle exposures is poorly understood. Direct toxicological evidence linking emitted NP to health effects is limited, but circumstantial evidence continues to grow. Several studies have shown that employment in (in lieu of exposures to) photocopy environments results in (moderately) increased levels of biomarkers of DNA damage in the peripheral blood of chronically exposed workers compared with controls (Manikantan et al. 2010; Balakrishnan & Das 2010; Gadhia et al. 2005, Goud et al. 2004, 2001). Shlomo and Shoenfeld (2008) reported on the development of anti-phospholipid syndrome (an autoimmune disease) on two individuals who had operated and serviced photocopy machines for several years. Theegarten et al. (2010) reports on an interesting case study implicating nanoparticle emissions from printers. In a recent study by our group (Khatri et al. 2012), it was found that several markers of inflammation (inflammatory cells, total protein, pro-inflammatory cytokines) in the nasal lavage and urine (8-hydroxy-2′-deoxyguanosine) samples collected from healthy volunteers exposed for 6 hours in a photocopy centre increased 2- to 10-fold compared with pre-exposure levels (Khatri et al. 2012). Tang et al. (2012) investigated the cytotoxicity and genotoxicity of laser printer emissions in human A549 lung cells using an air-to-liquid delivery system. They found that emissions of two out of five printers were genotoxic and that chemical composition more so than emission characteristics was the driving force behind such effects. The focus is shifting from investigating the toxicology of toners to that of nanoparticles.

The physicochemical composition of airborne PM fractions emitted from photocopiers remains poorly characterised. Nearly all health studies to date (with minor exceptions, e.g. Tang et al. 2012) share several limitations, more notably lack of quantitative exposure assessment and limited physicochemical and morphological characterisation of airborne PM. In addition, toxicological evaluation is limited to the use of toner particles (Bai et al. 2010) or organic solvent extracts (Gminski et al. 2010), rather than the emitted airborne PM. Proper characterisation of the chemical composition of such emissions is critical for routine exposure assessment and toxicological evaluations. Considering the complex toner chemistry (Supplemental material, Table SI) and the photocopying process, it is conceivable that airborne emissions may also include toner particles, volatile and SVOCs originating from the toner and other components (e.g. developer, fuser oil, plastic housing or paper). Bai et al. (2010) reported that toner particles they analysed contained ~200 nm size Fe_3O_4. Chemical analysis revealed that in addition to iron (30% by mass), the toner also contained other transition metals, including manganese (Mn, 1200 μg/g), Cr (800 μg/g) and Zn (188 μg/g). Similarly Gminski et al. (2010) found 3–30% iron as Fe_3O_4 in three toners, up to 7.6% Si, which contained traces of crystobalite (a polymorph of crystalline silica) and traces of other metals (Ni, Zn). They reported toner particles covered with particles in the 30–200 nm, and they contained Fe-rich nanoparticles. Similarly, Barthel et al. (2011) also reported that toners were rich in iron and contained smaller amount of several other metals (Si, Ti, V, Cr, Mn, Ni and Zn).

This study had two main objectives: (1) to characterise the physico-chemical and morphological properties of the airborne PM generated during the photocopying process, with particular emphasis on the nanoscale fraction. This characterisation was done in support of ongoing cytotoxicity and animal instillation studies, as well as to provide a basis for explaining the inflammatory and oxidative stress responses observed in humans (Khatri et al. 2012). (2) To establish that the properties of the emitted nanoparticles were related to the photocopying process and, more importantly, linked to the nanoparticles present in the toner formulation. Because realistic sampling was deemed important, we chose to sample in a real-world photocopy centre. Particles were tracked from the toner to the copier's exhaust filter to the indoor air environment. To our knowledge, this is the first 'real-world' physicochemical characterisation of nanoparticles emitted from photocopiers.

Methods

Facility description

Sampling took place in a university photocopy centre environment. The layout of the photocopy centre and a description of its activities, including photocopy volume, are presented in the supplemental material, Figure S1, and the accompanying text (facility description). The centre houses two high-volume photocopy machines from one major brand. Both machines use monochrome toners (black and white). The photocopying volume varies within and

between days and seasonally, with the highest workload coinciding with academic semesters and exam periods. On busy periods, the centre would print on average 20,000 pages/day, with maximum single orders of 52,000 pages. Information on the toner contained in the material safety data sheets (MSDS) is summarised in the supplemental material Table SI.The toners were reported to contain resin (>60%), iron powder (5–25%), carbon black (CB, ~ 5%) and treated silica (<5%).

Characterisation of toner and airborne PM

Figure 1 summarises schematically the approach for detailed physicochemical and morphological characterisation of PM from the toner to the air. This includes (1) toner particles obtained directly from the toner cartridges of each photocopy machine; (2) the dust retrieved from the copier's disposable air filter; and (3) size-fractionated airborne PM.

Several real-time, imaging and high-sensitivity analytical techniques were utilised for this purpose. Real-time monitoring instrumentation for size distributions and total number concentration is important in documenting nanoparticle and/or submicrometre particle emissions, whereas ozone concentrations are important for human respiratory (especially upper airway) toxicology and possible chemical reactions of ozone with airborne nanoparticles. Monitoring for VOCs is informative in the context of emissions and human respiratory toxicology (e.g. upper airway inflammation). TEM imaging specifically was needed for assessing the morphology of airborne nanoparticles and other submicrometre particles, and whether engineered nanoparticles were present in the toner. Elemental composition targeted primarily several transition metals of toxicological relevance.

Airborne PM

A suite of real-time instruments and time-integrated sampling methods were used to measure size distribution and collect PM for post-sample physicochemical, morphological and toxicological analysis. These include the following:

Real-time PM instruments

Particle size distribution and number concentration of the generated aerosol were measured using a Fast Mobility Particle Sizer (FMPS Model 3091, TSI Inc.) and an Aerodynamic Particle Sizer (APS Model 3321, TSI Inc.). These instruments monitored a broad size range (5.6 nm to 20 μm), with a response time of 1 sec. A condensation particle counter (CPC 3007, TSI Inc.) was also used with a 1-sec response time to obtain measures of the total number concentration in the range of 0.01–~1 μm. The FMPS measures electrical mobility diameter, whereas the APS, aerodynamic diameter. All instruments were factory calibrated and they all passed the field 'zero' calibration test with an online HEPA filter.

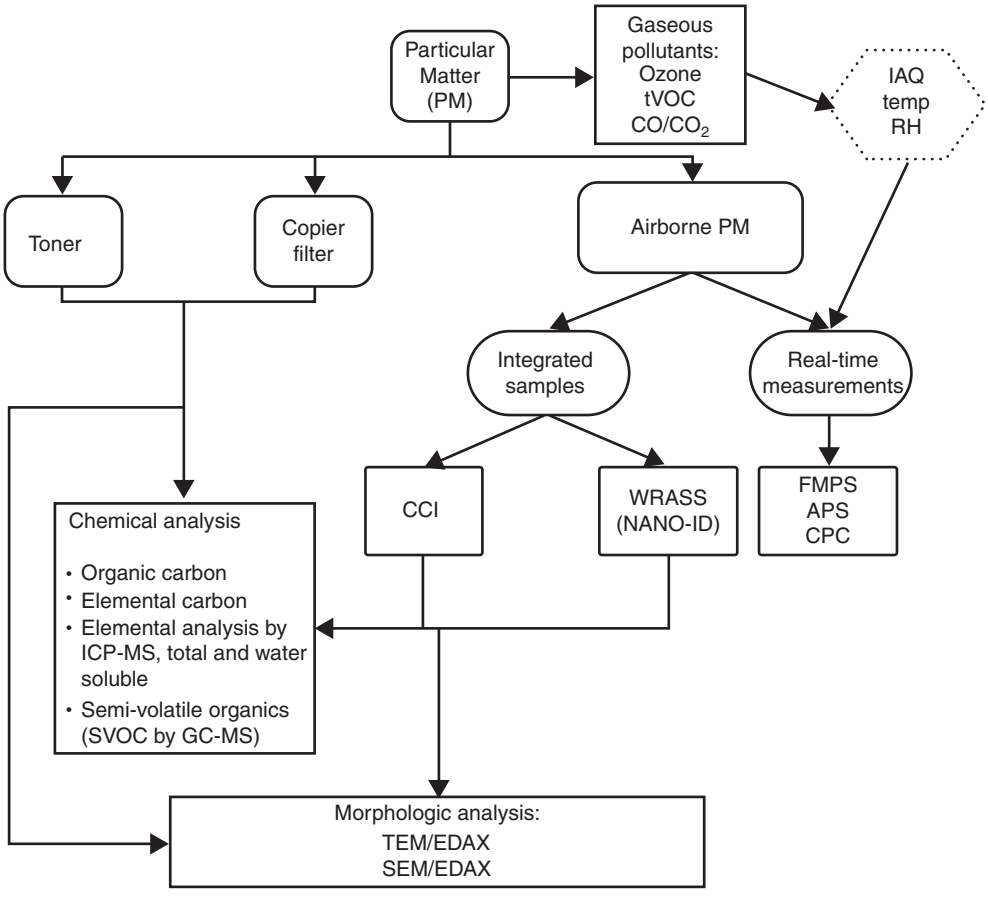

Figure 1. Schematics of the sampling approach.

Morphological analysis

A thermophoretic precipitator (TP, Fraunhofer Institute of Toxicology, Germany) and an electrostatic precipitator (ESP, Spokane Laboratories, NIOSH, WA) were used to collect particles directly onto transmission electron microscopy (TEM) grids for electron microscopy analysis. Sampling time varied between 1 and 8 min. The TEM grids (100- or 300-mesh copper with carbon film, Electron Microscopy Sciences, Hatfield, PA) were analysed by TEM (Philips EM 400T and the high-resolution Topcon 002-B) for particle size and morphology. Elemental analysis for particles of interest was obtained with the integrated energy dispersive spectroscopy (EDS) detector on the Topcon TEM. A total of six TEM grids were collected 10 cm from the exhaust port of the machines for aerosol morphological characterisation during peak emissions, as monitored in real time with the FMPS/APS/CPC 3007 instruments.

Size-selective integrated sampling of airborne PM

Two time-integrated PM samplers were used to sample size-fractionated airborne PM for chemical analysis: the Harvard Compact Cascade Impactor (Harvard CCI, Demokritou et al. 2004) and the Nano-ID (Naneum Ltd., UK; Gorbunov et al. 2009).

In this study, the Harvard CCI was operated with three stages and the final filter, corresponding to the $PM_{2.5–10}$ (coarse), $PM_{0.1–2.5}$ (fine) and $PM_{0.1}$ (nano, final filter) fractions and operates at 30 L/min. A 47 mm back-up Teflon membrane filter is used downstream of the last stage to collect particles smaller than 0.1 μm (nano or ultrafine PM fraction). The major feature of this novel sampler is its ability to both fractionate by size and collect relatively large amounts of particles (milligram quantities) onto inert polyurethane foam impaction substrates without the use of any adhesives (Salonen et al. 2000). The air flow rate was checked daily (AM and PM) using a mass flow meter (4100 series; TSI Inc.).

The Nano-ID operates at 20 L/min and consists of a cascade impactor for the upper seven stages (0.25–20 μm) with glass slides as collection media, and a diffusion battery for the lower five stages (2–250 nm) with mesh nets collection media. The glass slides were pre-cleaned with methanol and used without further surface pre-treatment. The diffusion battery was used only with stage 8 (Teflon filter, <250 nm) to maximise the amount of NM collected on a single filter for chemical analysis. More details about this sampler can be found in Gorbunov et al. (2009). Of note, the diffusion battery collects particles based on the diffusion-equivalent diameter (i.e. the mobility diameter), whereas the cascade impactor based on the aerodynamic diameter. The flow rate was checked twice a day (AM and PM) using the built-in flow meter.

Integrated sampling was conducted only during the work hours (7 AM–3 PM) and lasted typically 2–3 weeks per sample during November 2010–February 2011. The instruments were not turned on the days without any photocopying activity (to avoid oversampling of any background aerosols). Four side-by-side pairs of CCI and Nano-ID samples were collected during this time. Two of these pairs (CCIs) were used for subsequent chemical analysis (total and water-soluble metals and SVOCs). For each sampling campaign, one field blank was also collected. One Nano-ID sample was used for the organic and elemental carbon analysis (described later). Another Nano-ID sample was used for exploratory morphological and elemental analysis of individual stages. Field observations noted timing of instrument operation, photocopying activity and potential interfering PM sources.

PM (dust) sampled from copiers exhaust filter

Dust was collected straight from the copier's disposable air filter at the machines' exhaust port using SEM-compatible carbon tape. The collected PM was used in SEM/EDS for physicochemical and morphological analysis. Similarly, large visible amounts of deposits of dust in front of the filter housing could be easily wiped off and collected into pre-cleaned vials for chemical analysis.

Post-sampling physicochemical and morphological analysis of PM

Gravimetric analysis

The mass of collected PM on the PUFs (CCI) and Teflon filters (CCI and Nano-ID) was determined as mass difference between post- and pre-sampling weights of the substrates following 48 h of equilibration time in a temperature (20°C ± 1) and humidity controlled (50% ± 2) environmental chamber using a Cahn C-30 microbalance (Cahn Instruments, Cerritos, CA; 1 μg resolution). Weighing of the substrates was repeated if the mass difference of control blank filters was greater than 5 μg. The Nano-ID glass slides were wiped with a pre-weighed (and pre-baked) quartz filter punch (1 × 1 cm), and the mass of collected PM was determined by weight difference as above. The gravimetric limit of detection, determined as three times the standard deviation of repeated blank filter weights, was estimated at 3 μg and the limit of quantitation (three times the limit of detection) at 10 μg.

Chemical analysis

Chemical characterisation of the sampled airborne size-fractionated PM, toner and PM on the copier's disposable air filter, included elemental analysis for total and water-soluble metals; over 100 SVOCs, and organic and elemental carbon. Each analysis is described in more detail in subsequent sections as follows:

Elemental composition – magnetic sector ICPMS analysis

The total elemental composition of the PM samples (airborne fractions, toner, exhaust filter) was determined by magnetic-sector (SF) field inductively coupled plasma mass spectrometry (SF-ICP-MS) as described in Herner et al. (2006). For the Teflon-filter samples (ultrafine PM), toner and filter exhaust dust, samples were dissolved in a mixture of concentrated, high-purity acids (1.0 mL of 16N nitric acid, 0.1 mL of 28N hydrofluoric acid and 0.25 mL of 12N hydrochloric acid) in Teflon bombs with a programmable microwave digestion unit (ETHOS, Milestone). Digestates were diluted to 15.00 mL with high-purity water

(18 MΩ cm^{-1}) and stored in low-density polyethylene bottles, pre-cleaned in 2.4 N hydrochloric acid for 48 h, 3.2 N nitric acid for 48 h and rinsed with milli-Q high-purity water (Millipore, Bedford, MA). For PUF-collected samples (fine and coarse PM fractions), the procedure was similar, except that the acid matrix was a mixture of 1.5 mL of 16 N nitric acid (Optima grade, Fisher Scientific), 0.1 mL of 28 N hydrofluoric acid (Ultrex grade, J.T. Baker), 0.38 mL of 12 N hydrochloric acid (Optima grade, Fisher Scientific) and 0.50 mL of hydrogen peroxide; digestates were diluted to 30.00 mL. Water-soluble species in the PM were extracted with high-purity water (15.00 mL in acid-washed polypropylene tubes for 6.00 h with continuous shaking in the dark). The extract was filtered at 0.45 μm using acid-leached polypropylene syringe filters.

The digestates/extracts were analysed for 48 elements by SF-ICPMS (Thermo-Finnigan Element 2). Quality assurance samples in each analysis batch included sample spikes, sample duplicates, check blanks and standards, and a set of certified environmental matrix reference materials (NIST 2709, NIST 1648a, NIST 2556, NIST 2702). The analytical uncertainties were determined by sum-of-squares propagation of the uncertainty of the SF-ICP-MS measurement (standard deviation of three replicate measurements), the uncertainty of the method blank (standard deviation of 4–5 batch-specific blanks) and an estimate of the uncertainty in the digestion method (long-term standard deviation of replicate analyses of NIST Standard Reference Materials.

Semi-Volatile Organic Composition (SVOC) – GC/MS analysis

PM samples (airborne fractions, toner, exhaust filter) were analysed for more than 100 SVOCs by Soxhlet extraction-GC/MS (Stone et al. 2008). Substrates were spiked with a deuterated internal standard mix and then extracted using a 50:50 mixture of high-purity dichloromethane and acetone for 24 h. The solvent mixture was reduced in volume to approximately 4 mL using a rotary evaporator, filtered using an Acrodisc syringe filter and then blown down to approximately 1 mL using a gentle nitrogen stream. The samples were then subsequently blown down in a conical vial to a final volume of ~300 μL and derivatised with ~50–100 μL diazomethane solution and analysed on the GC/MS (Agilent 6890N Gas Chromatograph with 5973 inert MSD, and HP-5MS 30 m × 0.25mm ID × 0.25 μm column). The organic species quantified included PAHs, n-alkanes, n-alkanoic acids, resin acids, hopanes and steranes, and levoglucasan (Zheng et al. 2002).

Organic and elemental carbon (OC/EC)

Samples for elemental and organic carbon (EC-OC) analysis were collected on pre-baked quartz fibre filters (Turpin et al. 2000). The EC-OC were measured using the protocols standardised for the ACE-Asia intercomparison study (Schauer et al. 2003), which is a modified version of the NIOSH 5040 method that uses a Sunset Laboratory Inc. (Forest Grove, OR) laboratory-based thermal-optical analyser.

Gaseous co-pollutants

In addition to PM characterisation, we also monitored in real time for gaseous co-pollutants, such as ozone (Model 205, 2B Technologies Boulder, CO) and total VOCs (ToxiRae Plus photoionisation detector, RaeSystems, San Jose, CA). Other important indoor environmental quality parameters such as temperature, humidity, carbon dioxide and monoxide were monitored in real time using the Q-Trak Model 8550 and 7565 (TSI, Inc. Shoreview, MN).

Results

Aerosol size distribution and number concentration

Real-time sampling

Peak total number concentration of 2×10^5 with occasional excursions (on machine 2) over one million particles/cm^3 was commonly measured with highest levels measured at the exhaust filter ports and paper exit port. Continuous photocopying activity resulted in a significant increase in the total number concentration of nanoscale particles during the course of the working day as illustrated in Figure 2 and returned to indoor background levels only after midnight (data omitted).

Consistently we did not observe significant emissions of micrometre-sized particles, as illustrated in Figure 2C. Emissions were predominantly to nanoscale particles and exhibited broad peaks (6–100 nm) with the primary peak maximum in the 30–40 nm range, with another occasional peak below 10 nm (Figure 2B). Some variability in the size distributions was observed between each emission burst (i.e. high level intermittent exposures, <1 min duration) as illustrated in Figure 2B for each print job. Figure 2C shows that no appreciable amounts of large particles are being emitted. The total number concentration as measured by APS (particles with aerodynamic diameter greater than 500 nm) was a straight line at ~25 particles/cm^3 (graph not shown).

Ozone levels were low (5–20 ppb range, data omitted). The tVOCs were always below 0.1 ppm. The CO levels were always non-detectable (0.0 ppm) and the CO_2 levels varied in the 600–750 ppm range.

Integrated PM sampling

Mass size distribution of airborne PM for one side-by-side pair of the Harvard CCI and Nano-ID is presented in Figure 3. The mass distributions and concentrations were similar for the other pair. The average concentrations on each stage were in the 2–7 μg/m^3 and similar for both samplers. The highest concentrations were measured for the fine and ultrafine fractions: 7.1 μg/m^3 ($PM_{0.1-2.5}$) and 5 μg/m^3 ($PM_{<0.1}$) respectively. The calculated Nano-ID concentrations for these size fractions were 4.9 and 4.3 μg/m^3, respectively (Figure 3).

PM Morphological analysis

Toner PM

The morphology of toner 1 was characterized by irregularly shaped particles of ~5–20 μm (Figure 4A and supplemental material, Figure S2) suggesting that this toner was produced

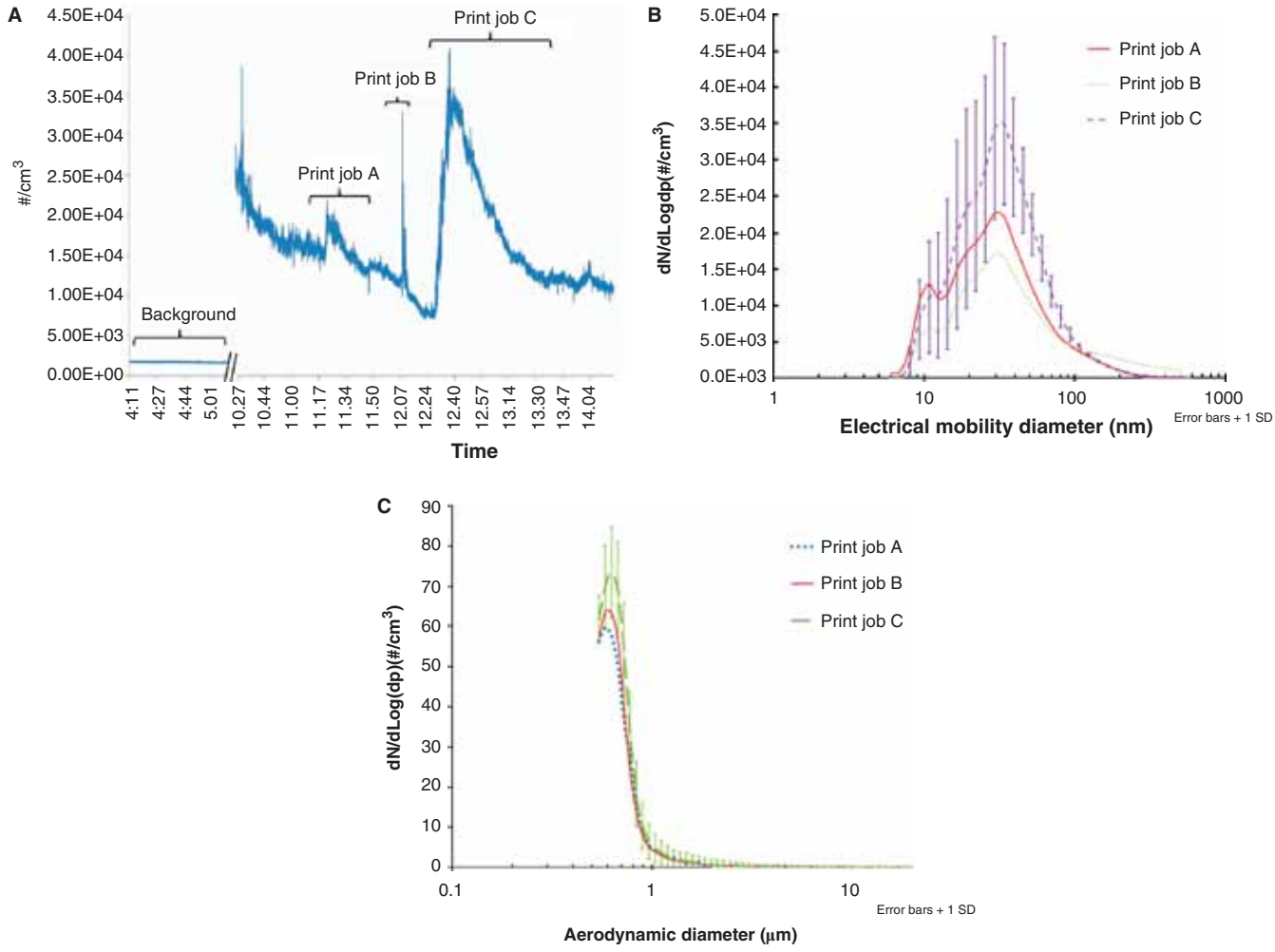

Figure 2. Photocopying leads to a significant increase in the concentration of nanoscale particles in the work environment over background levels as illustrated here for one day. Print job A, several small consecutive orders, 440 pages total; B, single order of 1320 pages; C, several large consecutive orders, 12,354 pages. A similar large order (8400 pages total) was completed between 8 and 10 AM of that morning. Note that much higher peak concentrations were measured on other days. 'A, FMPS, average size distributions of different printing jobs. Error bars (± 1SD) shown only for one distribution for clarity. C, APS, average size distributions for each print job (error bars (1 SD) shown only for one distribution for clarity). Total number concentration was flat at ~25 particles/cm^3'.

with conventional mechanical milling technologies. The second toner (Supplemental material, Figure S2) had more regular spherical particles in similar size ranges (indicative of emulsion aggregation technology, a wet chemistry method). Both toners were coated with aggregates of fumed silica nanoparticles of a broad size range, the only difference between them being the density of surface coverage. Toner 1 particles were fully coated (Figure 4A), whereas toner 2 particles had a lighter surface coating (supplemental material, Figure S2).

PM from Copier's exhaust filter

Selected representative images of particle morphologies of the dust tape stripped from the exhaust filter are shown in supplemental material (Figure S3). The dust was a complex mixture of different morphologies and particle sizes. Microscopic cellulose fibres of hundreds of micrometres in length and several micrometres in diameter were abundant. Predominant also were intact or fragmented toner particles and large amounts of salt crystals of different morphologies (Supplemental material Figure S3). The image in Figure 4B (albeit uncommon), which shows a drastically scarred surface, may provide clues to the processes that result in the generation of such nanoparticles. Agglomerates of nanoscale amorphous silica are visible on the surface of the particle.

Airborne PM

In contrast to the predominantly microscopic particles of the toner, other additives (such as developers, adhesion and charge additives, electric charge control agents, fluidising agents) were found on the PM collected from the exhaust port filter. Select representative images of nanoparticles collected at the source are shown in Figure 4C through E. The most predominant morphologies are shown in Figure 4C (regular round shape, ~10–80 nm in size) and Figure 4D (oil-like droplets), with sizes in good agreement with the FMPS measurements. Reliable energy dispersive analysis (EDS) of nanoparticles on Figure 4C and D was not possible due to their small size and evaporation under the high vacuum and high energy of the 200 keV TEM. The EDS of such nanoparticles yielded mostly carbon trace. However, there was also a smaller population of nano- (Figure 4G–H),

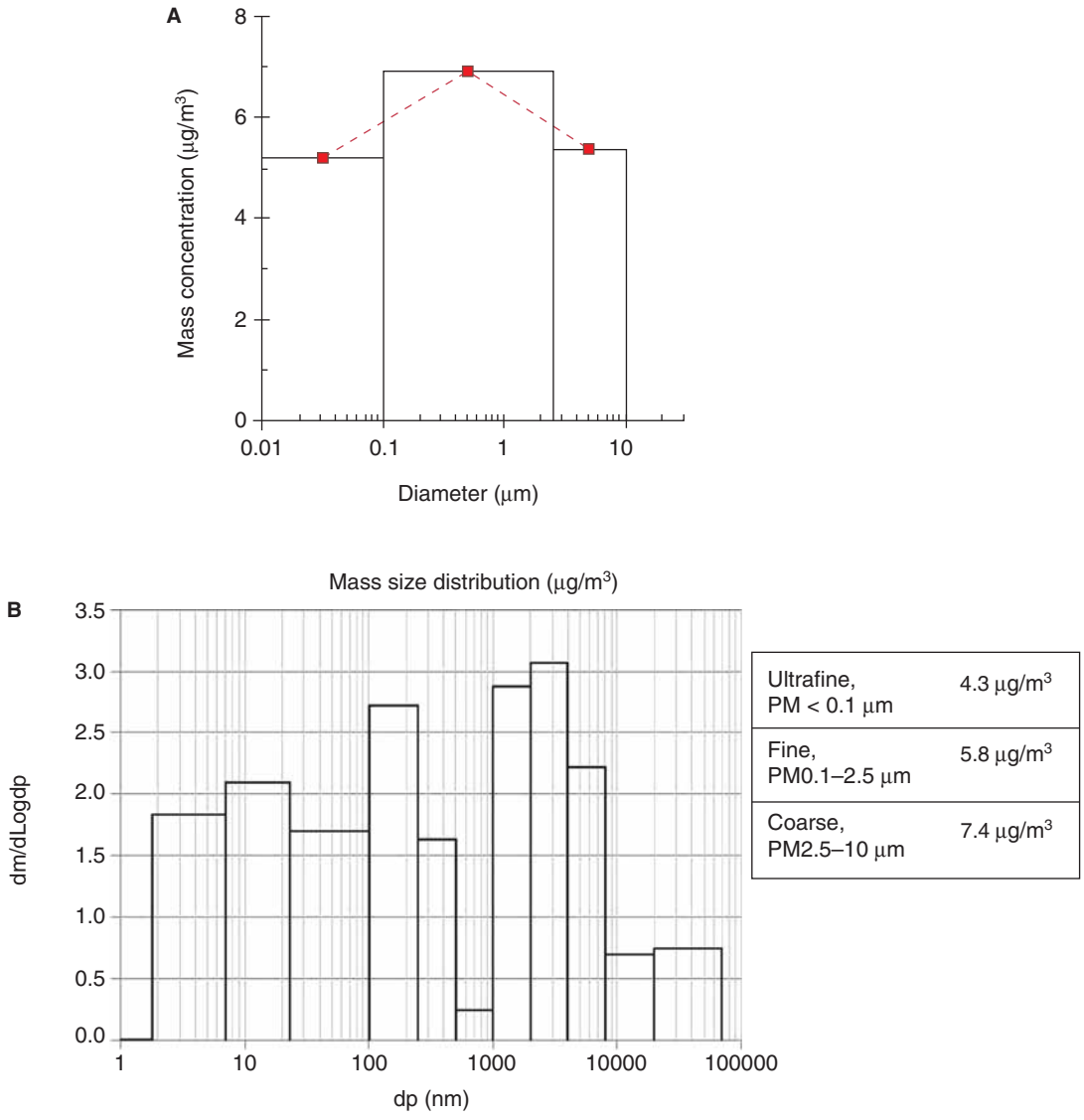

Figure 3. Size-selective mass distribution of airborne particulate matter derived from the Harvard Compact Cascade Impactor and the side-by-side Nano-ID.

submicrometre (Figure 4D–E) and microscopic particles (Figure 4F), which left behind a core rich in several metals, including Fe, Ti, Mn, Cr, Ni and Si (Figure 4), and other simpler EDS spectra (Supplemental material, Figure S4).

Chemical analysis

Organic and elemental carbon

Results of organic and elemental carbon analysis for both toners and size-fractionated airborne PM are presented in Figure 5. Toner 1 comprised 74% OC and 5.9% EC. The composition of toner 2 was similar (77.4% OC, 5.6% EC). Each toner contained 20% (toner 1) and 17% (toner 2) of other (inorganic) additives, such as metal oxides and salts. Due to substrate incompatibility, the OC/EC analysis could not be conducted on the CCI sampler and was instead conducted on the Nano-ID sample, collected size-by-side with the CCI as detailed in the methods section. The elemental carbon content in all of Nano-ID stages was negligible, ranging between 0.0% and 1.3%. The two submicrometre stages (no. 8, 2–250 nm and no. 7, 250 nm–1.0 µm) contained 0.1% and 1.3% elemental carbon, respectively. The relative amount of organic carbon in each of these stages was 49.8% and 70%, respectively. Larger particle size ranges contained between 40% and 70% OC. Over 99% of carbon in all stages was organic. Between ~29% and 59% of the collected aerosol mass on each stage was inorganic in origin.

Elemental analysis

The ICP-MS analysis results are presented graphically in Figure 5A through D and summarised in Table I. Toner 1 contained iron (Fe, 6%), titanium (Ti ~1%), silicon (Si, 2.8%), equal to ~6% SiO_2) as well as small amounts of manganese (Mn, 0.01%) and sulphur (S, 0.03%). Toner 2 contained Fe (2.4%) and Ti (0.4%), and higher levels of Mn (0.8%) and S (0.23%). Several other elements, including tin (Sn), aluminium (Al), zinc (Zn) and magnesium (Mg) were quantified in both toners in the 100–500 ppm range. All major metals in toners were poorly soluble in water (Fe, Ti, Mn and S). Si could not be analysed in the water extract of

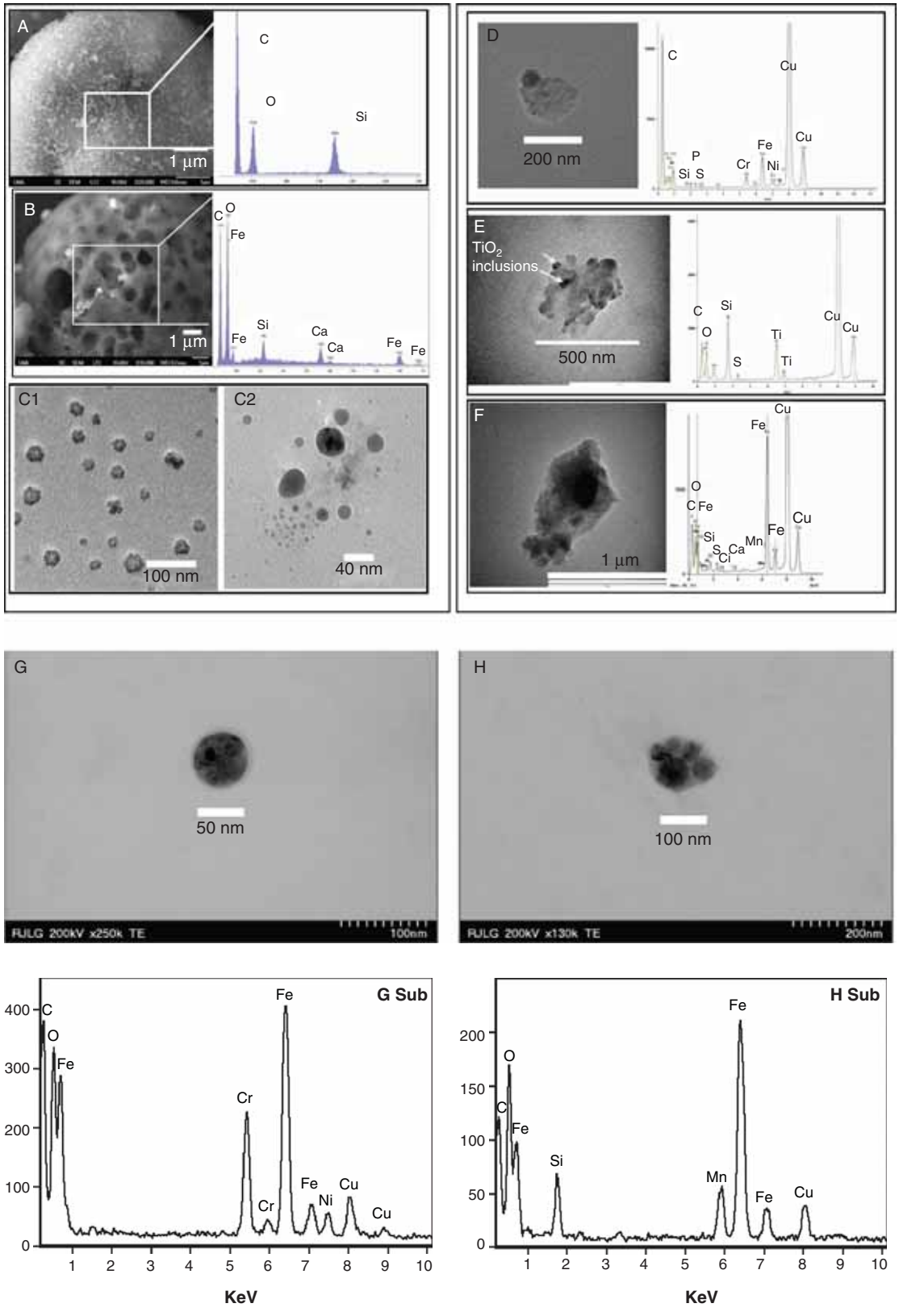

Figure 4. Representative morphological images of the toner surface (A, and its EDS), exhaust filter particles (B, and its EDS) and airborne PM (C1, C2, D–H and their EDS. The Cu signal comes from the Cu grid).

the toner; however, fumed silica is also not readily water soluble.

The exhaust filter PM contained Si (6.1%), Ti (3.5%), Ca (3.0%), Fe (1.5%), Al (0.4%), Na (0.4%), S (0.2%), Zn and Mg, at ~0.1% each, and ppm levels of several other metals, including Cr (400 ppm), Ni (380 ppm), Mn (185 ppm) and Sn (135 ppm). The exhaust filter PM was not analysed for OC/EC. The more abundant elements (Fe, Ti, Al) and some other transition metals (Cr, Ni, Mn, Sn) exhibited low water solubility (0.1–5%). Calcium and S were among

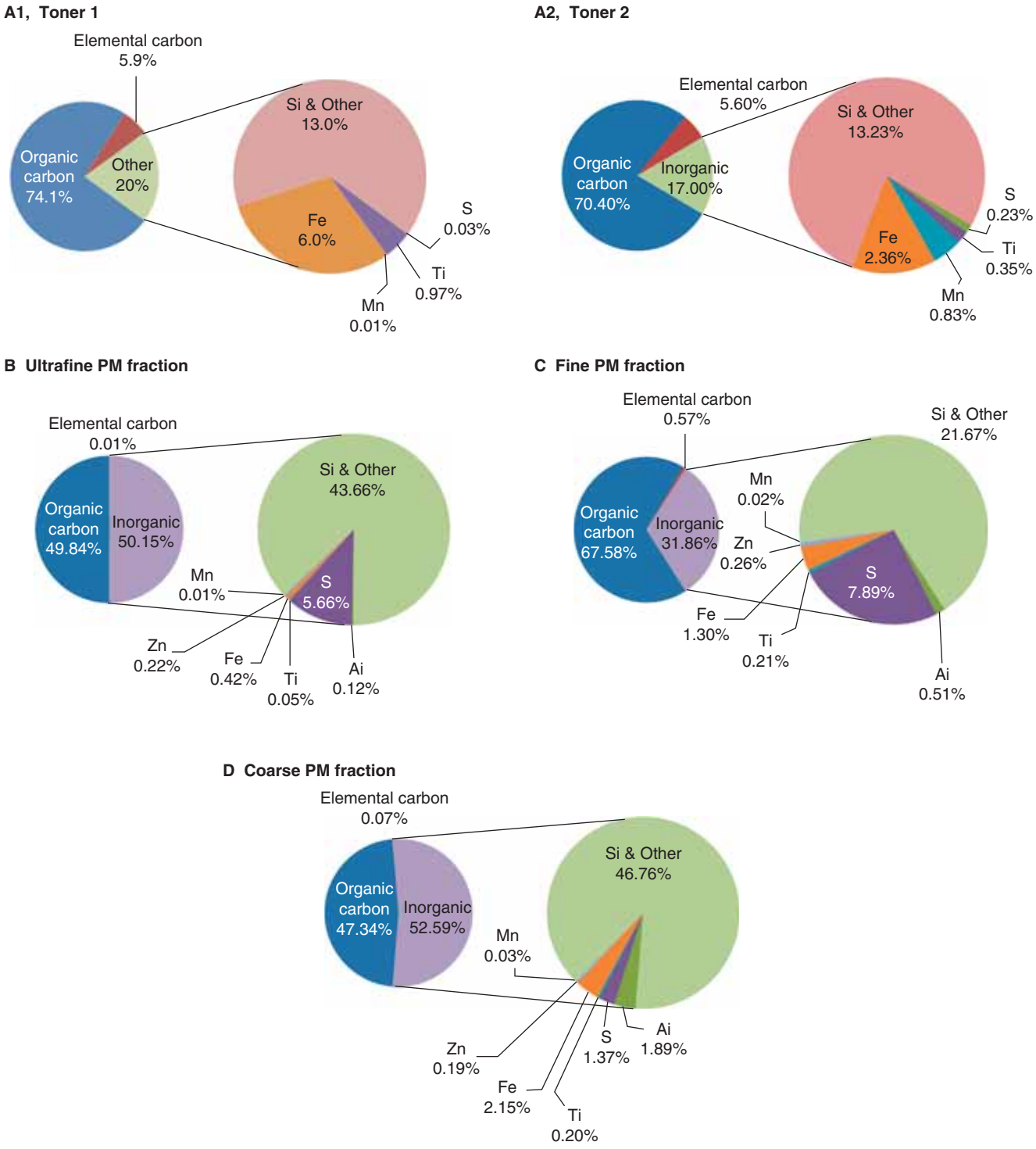

Figure 5. Elemental composition of toners and airborne particulate matter emitted from photocopiers. A1, toner 1; A2, toner 2; B, nanoscale fraction, PM < 0.1; C, fine PM fraction, PM 0.1-2.5; D, coarse PM fraction, PM 2.5-10.

the more water-soluble elements, at 29% and 34%, respectively.

The airborne PM contained a significant amount of organic carbon as well as inorganic content, which included all primary elements identified in the toners and the exhaust filter PM (Fe, Si, S, Ti, Mn, Al, Zn, Sn, P, Mg, Ca). Note that partitioning calculations of OC, EC and others in the left-side pies of Figure 5B–D are based on the matched Nano-ID sample, whereas the emerging pies to the right are based on ICP-MS analysis of the Harvard CCI sampler. These two samplers were matched (i.e. operated side by side for the same amount of time) and their size distributions were similar (Figure 3). The OC content of the airborne ultrafine PM accounted for 50%, with the other 50% being inorganic in nature. Of this 50% inorganic material, the most abundant elements were S (5.7%, 0.35 μg/m^3), Fe (0.42%, 0.02 μg/m^3) and Si (0.6%, 0.04 μg/m^3, see below). Other metals were present in small amounts, 1% or less: Zn (0.22%), Al (0.12%),

Table I. Magnetic sector inductively coupled plasma mass spectrometry (SF-ICP-MS) analysis of toners, exhaust filter dust and airborne size-fractionated particulate matter collected with the Harvard Compact Cascade Impactor (CCI). Elemental analysis targeted 47 elements. Only signature elements are presented here. Other elements of toxicological relevance (V, Co, As, Cd, Pb) were between 1-50 ppm. Other elements detected were Li, B, Na, P, K, Ca, Mg, Sc, Rb, Sr, Y, Nb, Rh, Pd, Ag, Sn, Sb, Cs, Ba, La, Ce, Pr, Nd, Sm, Eu, Dy, Ho, Yb, Lu, Pt, Th, U.

Sample	Element	Fe	Ti	Si[a]	Mn	Al	Zn	S	Cu	Cr	Ni	Mo
Toner 1	Total μg/g (SD)	59,964 (3748)	9692 (728)	28,290 (780)	66.8 (4.6)	13.6 (4.4)	220 (28)	257 (26)	87.5 (4.8)	27 (2.8)	37 (3.2)	2.1 (0.2)
	% Water soluble	0.0	0.0	n/a	0.1	8.6	87	36	-[b]	0.1	0.4	4
Toner 2	Total μg/g (SD)	23,591 (1502)	3549 (267)	9888 (325)	8325 (469)	584 (1.5)	6.3 (14.2)	2266 (201)	4.84 (0.6)	17.8 (1.1)	4.4 (0.5)	17 (1.7)
	% Water soluble	0.6	0.0	n/a	0.3	0.3	-	24	-	0.3	5.5	0
Exhaust filter dust	Total μg/g (SD)	14,998 (358)	3522 (27)	60,986 (11,676)	187 (3)	3523 (42)	1013 (31)	2000 (76)	576 (17)	436 (2)	382 (12)	36.6 (0.8)
	% Water soluble	0.05	0.01	n/a	4.3	4.2	3.0	34	3.3	0.25	2.4	2.9
Nanoscale (PM <0.1)	Total ng/sample (SD)	2025 (101)	262 (117)	2633 (1240)	45.8 (2.7)	632 (32)	1066 (56)	27,239 (1292)	132 (7.9)	18.3 (1.2)	46.6 (2.6)	17.7 (0.8)
(m = 0.461 mg)	% Water soluble	9	93	n/a	49	8.1	98	101	45	20	51	57
Teflon blank for PM <0.1	Total ng/filter (SD)	3.7 (2.7)	3.2 (1.1)	n/a	0.1 (0.1)	35 (7.5)	25 (22)	31 (18)	26 (1.4)	0.3 (0.4)	0.8 (4)	0.2 (0.1)
Fine PM (PM0.1–2.5)	Total ng/sample (SD)	8483 (486)	1484 (117)	12,660 (9100)	151 (8.6)	3394 (326)	1649 (116)	50,928 (4493)	420 (36)	73 (4.7)	94 (9.2)	41 (3.8)
(m = 0.651 mg)	% Water soluble	11.7	0.3	n/a	44	7.1	94	86	51	8.9	36	52
Blank for (PM0.1–2.5)	Total ng/filter (SD)	238 (31)	306 (26)	n/a	99.3 (5.3)	137 (35)	0 (19)	623 (56)	3.6 (4.4)	13.5 (1.1)	6.3 (0.4)	0.4 (0.4)
Coarse PM (PM2.5–10)	Total ng/sample (SD)	10,962 (611)	1068 (84)	-	153 (8.4)	9861 (864)	955 (61)	9199 (818)	349 (28)	102 (6.0)	68 (6.2)	16 (1.7)
(m = 0.497 mg)	% Water soluble	1.5	0.1	n/a	25	1.1	73	36	37	1.8	28	40
Blank for PM (PM2.5–10)	Total ng/filter (SD)	368 (60)	71 (11)	n/a	10.2 (0.8)	548 (81)	15 (38)	2464 (225)	41.8 (9.5)	60.3 (4.0)	28.6 (2.2)	1.6 (0.7)

[a]Silicon is an estimate based on reanalysis of initial digests and it is likely to be underestimated in some fractions. Values have been corrected for recovery; n/a, not analysed; [b]Soluble % not significantly different from zero.

Ti (0.05%), Sn (0.01%), and Ca (0.23%). Manganese was present at 100 ppm (0.01%), phosphorus at 560 ppm (present at 15 ppm in the toners), Mg at 650 ppm, whereas Sn at 145 ppm (530 ppm in one toner). All these metals were orders of magnitude higher than the blank values (of Teflon filter) and the method's quantitation limit (Table I). The larger component of this pie, 42.5%, is not fully accounted for. Si is an element that requires special handling in the ICP-MS analysis, related to the fact that the strong hydrofluoric/nitric acid mixture used for digestion converts Si to the volatile SiF_4. A reanalysis for Si was performed on the initial sample digests after confirming 70% recovery of Si in the accompanying NIST standard reference material (San Joaquin Soil) used with this batch of samples. The Si data on the airborne PM is an approximation and likely underestimated. Si was measured at 2.6 μg (corrected for recovery), which corresponds to <0.6% in the ultrafine PM fraction. The sum of all other quantified metals not listed above accounted for <1%. The remainder mass difference is likely attributed to elements such as O and Cl in metal oxides and salts.

The pie chart related to the fine PM fraction is similar to the ultrafine, except that all metals were found in higher quantities. The fine PM fraction contained more OC and EC than the ultrafine fraction, 68% OC and 0.6% EC, and higher content of all metals: S (8%), Fe (1.3%) and Ti (0.2%). Other elements were Zn (0.26%), Al (0.5%), Mg (0.4%), P (0.75%) and Mn (0.023%). Si was estimated at 127 μg in this fraction (~19%). Sn could not be quantitated reliably in the PUF stages (fine and coarse PM) due to high background Sn levels, likely related to a tin-based catalyst used in the PUF foam manufacturing.

The coarse PM fraction contained 54% OC and 0.1% EC. Notable is the much smaller content of S (1.9%) compared with the fine and ultrafine fractions and the generally slightly larger amounts of most other elements, including Fe (2.2%) and Al (2.0). Other elements were present in the following concentrations: Zn (0.2%), P (1.0%), Mn (0.03%) and Ti (0.2%). Silicon in this fraction was estimated at 2.9 μg, equivalent to 0.9% (corrected for recovery).

Metals in the airborne PM were more water soluble than that in the toner (Table I). This is likely due to the much larger surface area of the airborne fractions compared with the toner and encapsulation of metals inside the toner particles. For example, Fe was 10% water soluble in the ultrafine and fine fractions, 1.5% in the coarse fraction and <0.05% in the toner. Similarly, water solubility of Mn decreased in a similar order: 49, 44, 27, 0% for ultrafine, fine, coarse and toner PM, respectively. Titanium and Al were minimally water soluble in all fractions, <0.3% and <8%, respectively. Sulphur exhibited a similar trend, albeit much higher water solubility: 100, 86, 36, 22% for ultrafine, fine, coarse and toner PM, respectively. Calcium and Zn were readily water soluble, 85–100% in all fractions.

Semi-Volatile Organic Composition (SVOC)

PAHs were not detected in any of the toners or blank Teflon filters (ultrafine stages, at the ppb level). Some Other PAH species (e.g. phenanthrene, fluoranthene, pyrene, chrysene

and benzo(b)fluoranthene) were detected in all airborne fractions at levels moderately higher (two to five times) than the blank PUF foams (data omitted). These levels were generally very low, typically 10–50 ppb. The picture was identical for hopanes – none present in the toners and Teflon filters – and only modestly above blank values for all size fractions and typically in the low teens ppb (data not presented).

Toners contained n-alkanes from tetracosane (chain of 24 carbon atoms) to tetracontane (chain of 40 carbon atoms) ranging in concentration from 10 to 2670 ppm (Table II), the most abundant being tetracontane, octatriacontane and hexatriacontane.

All alkanes found in toners were also quantitated in all airborne fractions. The highest concentrations were found in the ultrafine fraction, followed by the fine PM fractions in a similar order of abundance as in the toner and in a concentration range of <2–10 ng/m^3. Note also small amounts of other alkanes (C17–C23), not quantified in the toners.

Discussion

This is the first study to quantitatively report on physicochemical and morphological composition of airborne nanoscale and other PM fractions emitted by commercial-grade photocopiers. The study focused in only one photocopy centre, which operated only two machines from one major manufacturer. In spite of this, the study reveals several important findings, with direct implications for environmental health and nanotoxicology.

Given the general trend of the nanotechnology industry to utilise nanoscale particles in many product formulations, it was hypothesised in this study that engineered nanoparticles are being used in commercial toners. This is a reasonable hypothesis, given the fact that the use of NMs in toner formulations can be found in patent applications a few decades back (Hendriksma & VanRhijn 1982). In addition, recent studies report on engineered nanoparticles in toners in printers (Gminski et al. 2010). Yet the extent to which such engineered nanoparticles are being used across the whole photocopying industry and their types are not known. We found that both toner particles were coated with nanoscale fumed silica, and they contained nanoscale titanium dioxide (Figure 4A and Supplement Figure S2-b). Interestingly, iron oxide particles could not be imaged in the toners, in spite of their high concentration (2.4% and 6% respectively). Repeated analysis of toners by two microscopists in two different analytical laboratories yielded similar imaging results for iron, and both laboratories found the same amounts of iron by ICP-MS. Possible quenching of iron X-ray emissions by other elements has been hypothesised but not verified. In addition, we observed iron oxide nanoparticles embedded within toner fragments collected during emission bursts (Figure 4D, F and Figure S4-c, d). Further investigations are needed to expand the scope of this work and map out different types of nanoscale additives and accompanying impurities in a larger sample of commercial toners from different manufacturers in order to verify these findings and our hypothesis.

The chemical composition of emitted nanoscale particles in this case is complex, mixed phases and includes different classes: organics, inorganic additives, carbon black, at least two different types of engineered nanoparticles, and it reflects the complex chemistry of toners. As an illustration, several nanoscale and submicrometre particles were a blend of different metal oxides and organics (Figure 4D–F), whereas others did not contain any inorganic ingredients (Figure 4C2). Our chemical analysis of the toners for organic and elemental carbon and elemental analysis agreed well with the manufacturer's description in MSDSs. High organic content in the nanoscale fraction is expected based on the studies of emissions in printers (Morawska et al. 2009), the high organic content of toners and the primary hypothesis on the mode of formation of nanoparticles from printers (likely with photocopiers as well) being condensation of SVOCs. All airborne fractions contained 50–70% OC, which is substantial. Based on TEM imaging and particle behaviour under high-vacuum and high-energy electron beam, organic nanoparticles were also predominant, with rough estimates at around 90–95%. Targeted analysis of over 100 SVOCs, and especially of long chain alkanes, matched well with their content in toners (Table II). However, the overall mass contribution of all measured SVOCs to the organic nanoscale and fine PM fraction was modest (<2%), suggesting that the chemical composition of these SVOCs is more complex, and it is expected to depend on the chemical composition of the toner resin and other organic additives. As such, their chemical composition may also vary between different photocopy environments, as a function of toner manufacturer brands.

The inorganic composition of airborne nanoscale fraction is also interesting chemically and toxicologically. Inorganic additives, including engineered nanoparticles, apparently become airborne as documented by single particle analysis and the good match between elemental analyses of toners, dust from exhaust filer and airborne fractions. For example, the nanoscale and fine PM contained significant amounts of certain metals traceable to the toner, especially Fe, Si, Ti, Mn, Al, Zn and Mg. Other elements in these airborne fractions, especially Ca, Na and K, were found in larger quantities in the exhaust filter dust, suggesting other potential sources in addition to toners (e.g. the paper). Based on single-particle elemental analysis and the published literature on toner formulations, most of these metals (except Na and K perhaps) are added as metal oxides (Fe_2O_3, TiO_2, SiO_2, $CaCO_3$, Al_2O_3). As such they tend to be poorly water soluble, which was generally the case here (<0.1–5% solubility for toner and exhaust filter dust), as well as Fe, Ti and Al in the nanoscale fraction. Some metals however may be in the form of organometallic compounds (e.g. zinc stearate), in which case the metal is more readily water soluble. This could partially explain the high water solubility of Ca and Zn in the airborne fractions. Sulphur and Mn were also water-soluble elements. Mn was present in small amounts (ppm values). The high solubility of sulphur may be due to certain water-soluble sulphates originating from salts additives (significant amounts of Ca and S found in the filter exhaust dust) or other sources.

Table II. Size-Selective semi-volatile organic compound (SVOC) analysis of airborne particulate matter and toners: Alkanes.

	Toner (μg/g)		Airborne PM (ng/sample) Air volume = 180 m^3			Blank	
Analyte	1	2	Ultrafine ($PM_{<0.1\ \mu m}$) (0.504 mg)	Fine ($PM_{0.1–2.5\ \mu m}$) (0.830 mg)	Coarse ($PM_{2.5–10\ \mu m}$) (0.303 mg)	Teflon filter ($PM_{<0.1\ \mu m}$)	PUF (Fine and coarse PM)
Heptadecane	–[a]	–	–	15.2	45.8	–	22.0
Octadecane	–	–	–	10.2	53.6	–	25.0
Nonadecane	–	–	–	10.5	53.0	–	26.5
Eicosane	–	–	–	30.5	134	–	52.2
Heneicosane	–	–	–	43.9	181	–	67.8
Docosane	–	–	–	137	447	–	118
Tricosane	–	–	–	121	299	–	82.0
Tetracosane	31.0	34.3	–	200	428	–	55.0
Pentacosane	11.6	–	10.2	87	144	–	20.9
Hexacosane	30.6	35.6	29.5	141	158	11.1	21.6
Heptacosane	20.7	25.1	53.9	120	89.2	24.4	26.2
Octacosane	75.8	81.0	241	156	119	25.6	32.1
Nonacosane	28.6	43.9	132	147	90.4	32.3	24.3
Triacontane	166	134	418	160	101	38.0	27.2
Hentriacontane	32.5	68.8	221	201	95.3	37.0	24.9
Dotriacontane	356	180	564	168	133	47.0	25.5
Tritriacontane	34.1	53.3	105	103	103	37.5	21.8
Tetratriacontane	799	235	788	190	162	42.4	30.7
Pentatriacontane	31.4	38.0	–	36.1	78.1	–	–
Hexatriacontane	1640	282	1120	226	142	–	–
Heptatriacontane	40.9	–	–	–	56.6	–	–
Octatriacontane	2420	374	1180	314	155	–	–
Tetracontane	2670	480	956	337	155	–	–

[a]Analyte not present. Method detection limit is analyte specific and <1 ng/mg (ppm). These analytes were not present in any of the samples or blanks: Nonane, Decane, Undecane, Dodecane, Tridecane, Tetradecane, Pentadecane, Hexadecane, Decylcyclohexane, Pentadecylcyclohexane, Nonadecylcyclohexane, Squalane.

The toxicology of these mixed nanoparticle exposures has not been studied. Only two studies to date provide some insights into their toxicological potency and potential modes of action. As mentioned previously, Tang et al. (2012) have shown recently that certain printer emissions are capable of inducing genotoxicity *in vitro* and that the chemical composition was an important factor in these effects. Khatri et al. (2012) has shown that these exposures induce upper airway inflammation, measured as an increase in several pro-inflammatory cytokines and chemokines, total proteins and inflammatory cells in the nasal lavage of healthy volunteers, as well as increased 8-OH-dG in urine (oxidative stress marker) following a single-day exposure in this same copy centre, compared with pre-exposure. Induction of IL-6, IL-8, TNF-α, VEGF, IL-1β, MCP1 is evidence of the immunogenic properties of these nanoparticles (Khatri et al. 2012). These organic nanoparticles are likely to be important players in the observed biological responses; however, there are no other published toxicological data on the actual nanoparticles from photocopiers against which to compare our observations. Although several of these elements may be in small quantities, their co-presence in the mixture as water-soluble metals and insoluble metal oxide nanoparticles is toxicologically important. While toxicity of several ionic metal species is well documented, toxicity of metal oxides nanoparticles is not always, nor entirely driven by dissolved ion species, and the mode of action may differ between nanoparticles and their ions (Cho et al. 2012; Pietruska et al. 2011). The synergistic effects of different constituents, for example, certain organics with transition metals, cannot be always foreseen. Yet such interactions may play important roles in the toxicity of such mixtures. For example, Guo et al. (2009) showed that co-exposures of carbon black and Fe_2O_3 nanoparticles induced synergistic oxidative stress-mediated cytotoxic effects, which were significantly greater than the additive effects of exposures to either particle type alone. Trace metal impurities (Mn, Fe, Co, etc.) in nanoparticles may catalyse production of reactive oxygen species, whereas surface modifications may remodel cellular uptake, nanoparticle trafficking inside the cells and their mode of action, resulting in several-fold increase in their toxicity, including the relatively benign fumed silica nanoparticles (Limbach et al. 2007; Nabeshi et al. 2011; Napierska et al. 2010). The critical role of chemical composition, metal impurity catalysts and mixture effects are well known in the case of ultrafine particles from air pollution, diesel exhaust or cigarette smoke (Li et al. 2008; Terzano et al. 2010). Additionally, nanoscale TiO_2 has been classified as a potential occupational carcinogen by the National Institute for Occupational Safety and Health (NIOSH 2011) and carbon black is classified by the International Agency for Research on Cancer (IARC) as a Group 2B, possibly carcinogenic to humans, based on 'sufficient evidence' in animals and 'inadequate evidence' in humans (Baan 2007).

Therefore, it is premature at the present time to assume that nanoparticle emissions from photocopiers in entirety or its certain individual components are benign. Further in-depth investigations into the chemistry and toxicology of these mixed nanoparticle exposures are needed, especially across a larger number of photocopy centres and toner formulations.

Differences in the chemical composition and toxicological properties may also exist between different size fractions, especially nanoscale and fine PM, and need to be further investigated. The chemical composition of the three airborne PM fractions shared several similarities among each other and with the toner and points to different formation processes for the airborne PM. All PM fractions contained 50–70% organic carbon and small but quantifiable elemental carbon (0.01–0.6%). In addition, all size fractions contained major metals identified in toners and the exhaust filter PM. However, the distribution of OC, EC and metals varied with the PM fraction. The highest EC content in the fine PM fraction is consistent with microanalysis observations of toner fragments on TEM grids, exhaust filter PM and Nano-ID impactor stages. Some of the discrepancy in the mass distribution of organic (50%) and inorganic (50%) components in the nanoscale fractions and distribution based on particle analysis (>90% of particles being organic in nature) may be related to different densities of these materials, with most metal oxides being much heavier. In the fine PM fraction, which contains smaller numbers of larger toner fragments, the organic content resembles more that of the toner. The EC content is notably small, but it also increases from the nanoscale to the fine PM fraction, consistent with this hypothesis and particle imaging. Therefore, the fine PM fraction of such exposures, which may vary in concentration and composition across other photocopy centres, should not be overlooked.

The mode of formation of nanoparticles from photocopiers and their emission characteristics are of interest from an engineering control and product reformulation standpoint. Collective evidence from OC/EC analysis (small content of EC in all fractions and the smallest EC content in the nano fraction, 0.01%), microanalysis (morphology in Figure 4C and D suggestive of condensation processes) and the SVOC analysis confirming highest concentration of high chain alkanes in the nano fraction in a similar abundance order with that measured in toners supports condensation aerosol formation as a major process. In this regard, our data are in agreement with several observations on printers (Morawska et al. 2009; Wensing et al. 2009, 2008). However, other evidence suggests that heterogeneous nucleation also seems to be important. Supportive evidence in favour of this hypothesis include the following: (1) fifty percent of the nanoscale fraction mass was inorganic in nature and its signature composition matched that of the toner and filter exhaust dust (Fe, Si, Ti, Mn, Al, Mg, Zn, as well as Ca, Na and K); (2) even though significant amounts of alkanes in all airborne PM fraction were measured, their sum can explain only a negligible fraction of the total mass for each fraction, including the nanoscale fraction. In this regard, our data agree well qualitatively with the recent results of Barthel et al. (2011), who found Si, S, Cl, Ca, Ti, Cr and Fe as well as traces of Ni, Zn and Br in different size fractions of the aerosols emitted from printers. Our results indicate that emissions of inorganic nanoscale aerosols from

photocopy equipment are significant and that processes other than condensation of SVOCs may be prominent in photocopiers. More targeted research is needed to answer questions of origin of certain other pollutants (such as P) and relative contribution of different sources (e.g. paper, developer and plastic housing). There is little doubt though that the primary source of such nanoparticle emissions is the photocopying process, of which the toner chemistry is undoubtedly an important parameter. It is possible that such nanoscale aerosols may undergo ageing as a result of subsequent chemical reactions with ultraviolet light, ozone and other trace pollutants as it disperses away from the source. We do not know at present whether such phenomena take place and their extent, but they deserve further consideration.

Background air pollution represents an ever-present challenge in the study of emissions, chemical composition or toxicology of engineered or other incidental nanoparticles in workplaces or the environment. Sampling in realistic environments in the presence of background nanoaerosols raises an important question as to what extend these data are biased by the sampled background air. The contribution of background aerosol in our results was apparent with the presence of very low, but detectable, amounts of some PAHs, smaller chain alkanes (<20 carbons) and some hopanes in the nanoscale aerosol. Long-term average area particle number concentrations in this copy centre measured 2 m away from the sources (photocopiers) were at least eight times higher than long-term average background levels (Khatri et al. 2012). Because the samplers were located next to the source, the difference between background and area concentrations at the source were much higher, with mean number concentration ratio of 15. While background nanoaerosol may have biased some individual analytes, it is unlikely for it to have biased the overall picture reconstructed form multiple instruments and comparative analysis with the toners and the exhaust filter PM. Yet differentiation of background aerosol from photocopiers emissions in realistic environments is of special interest for routine exposure assessment studies. Our data suggest that analysis for OC/EC, metals and high chain alkanes, both in toners and airborne PM fractions, especially the nanoscale fraction, is highly informative. Future research may identify more specific exposure markers of nanoparticle emissions from photocopiers.

Chronic exposures to these environments may possibly lead to chronic diseases, as has been suggested by several previously mentioned studies. We believe that further in-depth investigations into the chemistry and toxicology of these exposures are needed. Such future studies should further address in more details the chemical composition of the organic fraction of the airborne PM, especially the nanoscale fraction, variability in toner formulations, the influence of paper quality and fuser oil, and other exposure-modifying factors such as copier characteristics, that is, fusion temperature, design specifications, capacity, cycle frequency and time and so on. In addition, further investigation is needed with regard to the potential sources of phosphorous and its link with flame retardants, as well as the origin of sulphur and other elements. Given the wide spread use of this technology and the scarce data, larger scale exposure assessment studies on nanoparticles in this industry sector are needed.

Conclusions

We investigated size-selective chemical and morphological composition of airborne PM in a commercial-grade photocopy centre. Our investigation reveals several new findings: (1) That several engineered nanoparticles (fumed silica, titania and possibly iron oxide) used in toner particles become airborne; (2) chemical composition of all airborne PM fractions, including the nanoscale fraction, is complex and contains all major elements and classes of analytes found in the toners, including metals, SVOCs, organic and elemental carbon, and points to different sources; (3) the organic fraction of the aerosol comprised 50–70% of the total mass and its chemistry, still not fully characterised, is likely to vary with the toner formulation. We conclude that further in-depth investigations into the chemistry and toxicology of these exposures are needed and that detailed quantitative exposure assessment studies on nanoparticles are necessary for evaluating occupational and consumer health risks related to this technology.

Acknowledgement

Authors would like to thank the photocopy centre employees for their help and support, as well as Dr. Earl Ada of the UML Materials Characterization Laboratory and Prof. Daniel Schmidt for their assistance with morphological analysis of toners and nanoparticles. This study was supported in part by the Nanoscale Science and Engineering Centers Program of the National Science Foundation (Award #NSF-0425826) NSF center Grants and the Center for Nanotechnology and Nanotoxicology at the Harvard School of Public Health.

Declaration of interest

The authors report no conflicts of interest. The authors alone are responsible for the content and writing of the paper.

References

Baan RA. 2007. Carcinogenic hazards from inhaled carbon black, titanium dioxide, and talc not containing asbestos or asbestiform fibers: recent evaluations by an IARC Monographs Working Group. Inhal Toxicol 19(Suppl 1):213–228.

Bai R, Zhang L, Liu Y, Meng L, Wang L, Wu Y, et al. 2010. Pulmonary responses to printer toner particles in mice after intratracheal instillation. Toxicol Lett 199(3):288–300.

Balakrishnan M, Das A. 2010. Chromosomal aberration of workers occupationally exposed to photocopying machines in Sulur, South India. Int J Pharma Bio Sci 1(4):B-303–B-307.

Barthel M, Pedan V, Hahn O, Rothhardt M, Bresch H, Jann O, et al. 2011. XRF-analysis of fine and ultrafine particles emitted from laser printing devices. Environ Sci Technol 45(18):7819–7825.

Cho W-S, Duffin R, Poland CA, Duschl A, JannekeOostingh G, MacNee W, et al. 2012. Differential pro-inflammatory effects of metal oxide nanoparticles and their soluble ions in vitro and in vivo; zinc and copper nanoparticles, but not their ions, recruit eosinophils to the lungs. Nanotox 6(1):22–35.

Demokritou P, Lee SJ, Ferguson ST, Koutrakis P. 2004. A compact multistage (cascade) impactor for the characterization of atmospheric aerosols. J Aerosol Sci 35(3):281–299.

Destaillats H, Maddalena RL, Singer BC, Hodgson AT, McKone TE. 2008. Indoor pollutants emitted by office equipment: A review of reported data and information needs. Atmospher Environ 42 (7):1371–1388.
Gadhia PK, Patel D, Solanki KB, Tamakuwala DN, Pithawala MA. 2005. A preliminary cytogenetic and hematological study of photocopying machine operators. Indian J Occup Environ Med 9(1):22–25.
Gminski R, Decker K, Heinz C, Seidel A, Könczöl M, Goldenberg E, et al. 2010. Genotoxic effects of three selected black toner powders and their dimethyl sulfoxide extracts in cultured human epithelial A549 lung cells in vitro. Environ Mol Mutagen 52(4):296–309.
Gorbunov B, Priest ND, Muir RB, Jackson PR, Gnewuch H. 2009. A novel size-selective airborne particle size fractionating instrument for health risk evaluation. Ann Occup Hyg 53(3):225–237.
Goud KI, Hasan Q, Balakrishna N, Rao KP, Ahuja YR. 2004. Genotoxicity evaluation of individuals working with photocopying machines. Mutat Res Genet Toxicol Environ Mutagen 563(2):151–158.
Goud KI, Shankarapppa K, Vijayashree B, Rao PK, Ahuja YR. 2001. DNA damage and repair studies in individuals working with photocopying machines. Int J Hum Genet 1(2):139–143.
Guo B, Zebda R, Drake SJ, Sayes CM. 2009. Synergistic effect of co-exposure to carbon black and Fe2O3 nanoparticles on oxidative stress in cultured lung epithelial cells. Part Fibre Toxicol 6:4.
He C, Morawska L, Taplin L. 2007. Particle emission characteristics of office printers. Environ Sci Technol 41(17):6039–6045.
He C, Morawska L, Wang H, Jayaratne R, McGarry P, Richard JG, et al. 2010. Quantification of the relationship between fuser roller temperature and laser printer emissions. J Aerosol Sci 41(6): 523–530.
Hendriksma RR, VanRhijn WJ. 1982. Dispersion-heat process employing hydrophobic silica for producing electrophotographic toner powder. United States patent # 4,345,015, August 171982.
Herner JD, Green PG, Kleeman MJ. 2006. Measuring the trace elemental composition of size-resolved airborne particles. Environ Sci Technol 40(6):1925–1933.
Kagi N, Fujii S, Horiba Y, Namiki N, Ohtani Y, Emi H, Tamura H, Kim YS. 2007. Indoor air quality for chemical and ultrafine particle contaminants from printers. Build Environ 42(5):1949–1954.
Khatri M, Bello D, Gaines P, Martin J, Pal AK, Gore R, Woskie S. 2012. Nanoparticles from photocopiers induce oxidative stress and upper respiratory tract inflammation in healthy volunteers. Nanotoxicology, manuscript ID: 691998. Accepted May 6, 2012. (ID: 691998 DOI:10.3109/17435390.2012.691998)
Lee C-W, Hsu D-J. 2007. Measurements of fine and ultrafine particles formation in photocopy centers in Taiwan. Atmospher Environ 41 (31):6598–6609.
Li N, Xia T, Nel AE. 2008. The role of oxidative stress in ambient particulate matter-induced lung diseases and its implications in the toxicity of engineered nanoparticles. Free Radic Biol Med 44 (9):1689–1699.
Limbach L, Wick P, Manser P, Grass RN, Bruinink A, Stark WJ. 2007. Exposure of engineered nanoparticles to human lung epithelial cells: influence of chemical composition and catalytic activity on oxidative stress. Environ Sci Technol 41:4158–4163.
Lövestam G, Rauscher H, Roebben G, Klüttgen BS, Gibson N, Putaud J-P, et al. 2010. Joint research commission reference report: considerations of a definition for regulatory purposes. Luxemburg: Publications Office of the European Union. doi 10.2788/98686.
Manikantan P, Balachandar V, Sasikala K, Mohanadevi S, Lakshmankumar B. 2010. DNA damage in workers occupationally exposed to photocopying machines in Coimbatore south India, using comet assay. Internet J Toxicol 7(2):1–9.
McGarry P, Morawska L, He C, Jayaratne R, Falk M, Tran Q, et al. 2011. Exposure to particles from laser printers operating within office workplaces. Environ Sci Technol 45(15):6444–6452.
Morawska L, He C, Johnson G, Jayaratne R, Salthammer T, Wang H, et al. 2009. An investigation into the characteristics and formation mechanisms of particles originating from the operation of laser printers. Environ Sci Technol 43(4):1015–1022.
Nabeshi H, Yoshikawa T, Arimori A, Yoshida T, Tochigi S, Hirai T, et al. 2011. Effect of surface properties of silica nanoparticles on their cytotoxicity and cellular distribution inmurine macrophages. Nanoscale Res Lett 6:93.
Napierska D, Thomassen LC, Lison D, Martens JA, Hoet PH. 2010. The nanosilica hazard: another variable entity. Part Fibre Toxicol 7(1):39.
NIOSH, National Institute for Occupational Safety and Health. 2011. Current Intelligent Bulletin 63: Occupational expusre to titanium dioxide. DHHS (NIOSH) Publication No. 2011–160.
Pietruska JR, Xinyuan L, Smith A, McNeil K, Weston P, Zhitkovich A, et al. 2011. Bioavailability, intracellular mobilization of nickel, and HIF-1α activation in human lung epithelial cells exposed to metallic nickel and nickel oxide nanoparticles. Toxicol Sci 124(1):138–148.
Salonen RO, Pennanen AS, Halinen AI, Hirvonen MR, Sillanpaa M, Hillamo R, et al. 2000. A chemical and toxicological comparison of urban air PM10 collected during winter and spring in Finland. Inhalat Toxicol 12(Suppl 2):95–103.
Schauer JJ, Mader BT, Deminter JT, Heidemann G, Bae MS, Seinfeld JH, et al. 2003. ACE-Asia intercomparison of a thermal-optical method for the determination of particle-phase organic and elemental carbon. Environ Sci Technol 37:993–1001.
Schripp T, Wensing M, Uhde E, Salthammer T, He C, Morawska L. 2008. Evaluation of ultrafine particle emissions from laser printers using emission test chambers. Environ Sci Technol 42(12):4338–4343.
Shlomo B-S, Shoenfeld Y. 2008. Photocopy machines and occupational antiphospholipid syndrome. IMAJ 10:52–54.
Stone EA, Snyder DC, Sheesley RJ, Sullivan AP, Weber RJ, Schauer JJ. 2008. Source apportionment of fine organic aerosol in Mexico City during the MILAGRO experiment 2006. Atmos Chem Phys 8:1249–1259.
Tang T, Gminski R, Könczöl M, Modest C, Armbruster B, Mersch-Sundermann V. 2012. Investigations on cytotoxic and genotoxic effects of laser printer emissions in human epithelial A549 lung cells using an air/liquid exposure system. Environ Mol Mutagen 53(2):125–135.
Terzano C, Di Stefano F, Conti V, Graziani E, Petroianni A. 2010. Air pollution ultrafine particles: toxicity beyond the lung. Eur Rev Med Pharmacol Sci 14(10):809–821.
Theegarten D, Boukercha S, Philippou S, Anhenn O. 2010. Submesothelial deposition of carbon nanoparticles after toner exposition: case report. Diagn Pathol 5:77–80.
Tuomi T, Engström B, Niemelä R, Svinhufvud J, Reijula K. 2000. Emission of Ozone and organic volatiles from a selection of laser printers and photocopiers. Appl Occup Environ Hyg 15(8):629–634.
Turpin BJ, Saxena P, Andrews E. 2000. Measuring and simulating particulate organics in the atmosphere: problems and prospects. Atmospher Environ 34:2983–3013.
Wensing M, Delius W, Omelan A, Uhde E, Salthammer T, He C, et al. 2009. Ultra-fine particles (UFP) from laser printers: chemical and physical characterization. Paper ID 171. In: Proceedings of the 9th International Conference on Healthy Buildings; Syracuse, NY.
Wensing M, Schripp T, Uhde E, Salthammer T. 2008. Ultra-fine particles release from hardcopy devices: sources, real-room measurements and efficiency of filter accessories. Sci Total Environ 407(1):418–427.
Zheng M, Cass GR, Schauer JJ, Edgerton ES. 2002. Source apportionment of PM2.5 in the Southeastern United States Using solvent-extractable organic compounds as tracers. Environ Sci Technol 36(11):2361–2371.

Supplementary material available online

Supplementary Table SI.
Supplementary Figures S1–S4.